A hybrid model for generating short-time g-functions

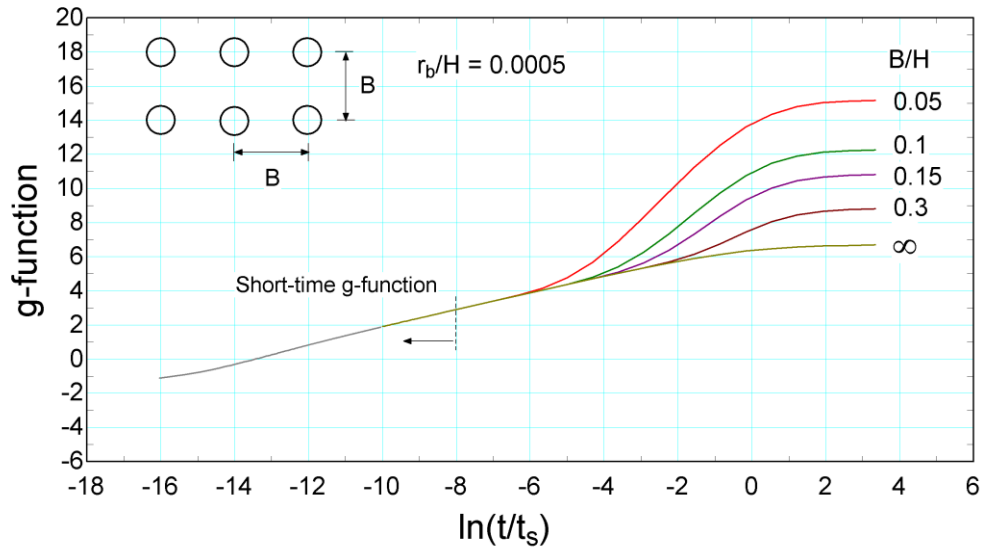**Yves Brussieux**   **Michel Bernier**

ABSTRACT

A hybrid numerical/analytical approach is proposed to predict short-time g-functions. Transient heat transfer in the borehole is solved numerically while ground heat transfer is evaluated analytically using the infinite cylindrical heat source solution. Grid independence checks indicate that 40 radial nodes and a time step of 3 minutes represent a good compromise between computational time and accuracy. The proposed model is successfully validated against test cases, which include transient heat transfer in a plane wall and experimental data from a sand box.

In the application section of the paper, the classic ASHRAE sizing equation is modified to account for borehole thermal capacity using short-time g-functions. It is shown that the inclusion of borehole thermal capacity has a direct effect on the daily and monthly effective ground thermal resistances which reduces the required borehole length by a few percent. It is concluded that borehole thermal capacity should be included when sizing a bore field.

INTRODUCTION

Heat transfer calculations from vertical ground heat exchangers (VGHE) are typically performed over two distinct regions, within the borehole and in the ground. In the ground, transient heat transfer from the borehole wall to the far-field is evaluated with thermal response factors such as g-functions (Eskilson, 1987). In the borehole, i.e. from the fluid to the borehole wall, calculations are typically performed using a steady-state borehole thermal resistance by neglecting the fluid and grout thermal capacity within the borehole. While the steady-state assumption in the borehole is valid when the borehole operates continuously, it is shown to be inaccurate for rapidly changing borehole inlet conditions (Shirazi and Bernier, 2013) or when sizing a bore field with a short peak pulse (Ahmadfard and Bernier, 2018).

It is possible to extend the traditional (so-called long-term) g-functions to short time-steps to account for borehole thermal capacity. Thus, with this unified g-function curve, heat exchange with the ground can be predicted over time scales ranging from minutes to decades. Examples of such curves are presented in Figure 1 for a 3×2 bore field geometry. This figure is constructed with five long-term g-function curves for five B/H ratios obtained using the techniques described by Cimmino and Bernier (2013, 2014) while the short-term g-function segment is determined with the model proposed in this paper. As mentioned by Yavuzturk and Spitler (1999), much of the original g-functions calculated by Eskilson (1987) did not cover time periods of less than a month. Yavuzturk and Spitler (1999) also mention that Hellström extended the g-functions so that they could be used down to about 100 hours. For a typical borehole, this represents a value of $ln(t/t_s) \approx$ -8. For lower values, it is necessary to account for transient effects in the borehole. In this paper, this is accomplished using short-time g-functions.

Yves Brussieux (yves.brussieux@polymtl.ca) is a graduate student and Michel Bernier (michel.bernier@polymtl.ca) is a professor of mechanical engineering at Polytechnique Montréal.

Figure 1   Short and long-term g-functions for a 3 × 2 bore field.

Yavuzturk and Spitler (1999) were the first to extend the concept of g-functions to short time steps taking into account the pipe and grout thermal capacities but neglecting the fluid thermal capacity. Xu and Spitler (2006) extended this work by approximating the U-tube geometry with a series of hollow cylinders representing the fluid, the internal convective resistance, the pipe, the grout and the ground. They have shown that results obtained with this technique compare favorably well with the ones obtained with a two-dimensional model representing the real borehole geometry.

Calculation methods to account for borehole thermal capacity were reviewed by Shirazi and Bernier (2013). Other studies which were not reviewed by these authors will now be briefly discussed.

Javed et al. (2010), Javed and Claesson (2011) and Claesson and Javed (2011) proposed an analytical one-dimensional model to simulate the short and long term thermal response of vertical ground heat exchangers where the U-tube is replaced by a composite cylinder. Borehole heat transfer is solved in the Laplace domain with the use of a circuit of thermal resistances and then inverse transforms are used to revert back to the time domain. Lamarche (2015) used a similar approach and later used his solution (Lamarche, 2016) to study the impact of short time effects on the required length of VGHE. He showed that for a particular case, the required borehole length could be overestimated by about 5% when short-term effects are neglected.

Li and Lai (2013) and Li et al. (2014) proposed a two-dimensional analytical models for U-tube boreholes in which each tube is replaced by an infinite line source. Their results match experimental data with good accuracy for times as short as several minutes. Ma et al. (2015) used a similar composite-medium line source but in three-dimensions to also account for the variation of fluid temperature along the U-tube. However, the fluid thermal capacity is not taken into account in these models. Yang and Li (2014) compared the composite-medium line-source analytical solution of Li and Lai (2013) with a new two-dimensional model using a finite volume approach. This model uses the same assumptions and also considers the influence of the fluid thermal capacity. It is shown that the results are very similar but a better estimation is made with the numerical model for the first few minutes.

Bauer et al. (2011) proposed a three dimensional model based on a thermal resistance and capacity network, however, such a degree of precision imply relatively high computational costs. Rees (2015) presents a two-dimensional model based on the finite volume method to allow for fluctuations of the fluid temperature along the U-tube. Kim et al. (2014) used a hybrid model, numerical inside the borehole and analytical in the ground, to account for borehole thermal capacity. They used an equivalent radius and a state model size reduction technique to limit computation time. Despite these simplifications, they show results quite similar to analytical models. Ruiz-Calvo et al. (2015) proposed a

model called Borehole-to-Ground (B2G) with a thermal network approach to evaluate the internal thermal resistance. This model accounts for grout and fluid thermal capacities and is also combined with long term g-functions (Ruiz-Calvo et al., 2016) to obtain a complete model. Parisch et al. (2015) accounted for the fluid and grout thermal capacities by adding an adiabatic pipe, which accounts for the borehole thermal capacity, upstream of a steady-sate borehole model. Simulations results in TRNSYS performed with this approach show significant improvements.

In the present work, a hybrid approach is proposed to predict short-time g-functions. First, the U-tube geometry is transformed into an equivalent composite cylinder using the approach suggested by Xu and Spitler (2006). Then, heat transfer from the fluid to the borehole wall is evaluated numerically using Patankar's (1980) finite volume approach. Finally, ground heat transfer is evaluated analytically using the infinite cylindrical heat source solution where the heat transfer rate at the borehole wall is obtained from the numerical solution.

After a presentation of the governing equations and the solution methodology, the paper addresses the issue of grid independence and makes recommendations on the number of required nodes and time-step durations to obtain accurate solutions. The approach is then validated against analytical solutions and experimental data. In the application section of the paper, the ASHRAE sizing equation for VGHE is used in conjunction with short-time g-functions to show the impact of borehole thermal capacity on sizing.

PROPOSED MODEL

The following model is based on the equivalent geometry proposed by Xu and Spitler (2006) and illustrated in Figure 2. The two-pipe geometry, with a borehole radius r_b, is converted into a composite cylinder configuration with the same borehole radius. The outer pipe radius of the equivalent geometry, $r_{eq,out,p}$, is set equal to $\sqrt{2}\ r_{out}$. This ensures that the volume occupied by the grout is the same in both the real and equivalent geometry. The inner pipe radius of the equivalent geometry, $r_{eq,in,p}$, is set equal to $r_{eq,out,p}$ minus the pipe thickness $\Delta\ (= r_{out} - r_{in})$. Then a mass-less convection layer with a thickness of $0.25 \times \Delta$ followed by a fully-mixed fluid layer with a thickness of $0.75 \times \Delta$ are used as suggested by Xu and Spitler (2006). An additional radius, r_{far} , is used by Xu and Spitler (2006) to set the far-field radius in the ground for their numerical model. This radius is not required here since ground heat transfer is handled with an analytical solution. An equivalent fluid thermal capacity, $\rho Cp_{eq,f}$, is determined based on the actual fluid thermal capacity, ρCp_f, as follows:

$$\rho Cp_{eq,f} = \frac{2r_{in}^2}{\left(r_{eq,in,c}^2 - r_{eq,f}^2\right)}\rho Cp_f \tag{1}$$

The local fluid is at a temperature equal to the average borehole fluid temperature, T_f, while the undisturbed ground temperature is given by T_g. The steady-state borehole thermal resistance, R_b, is equal for both geometries. It is determined here using the first order multipole method (Hellström, 1991) based on the real geometry. Once the value of R_b is known, each layer are assigned equivalent properties as shown in Table 1.
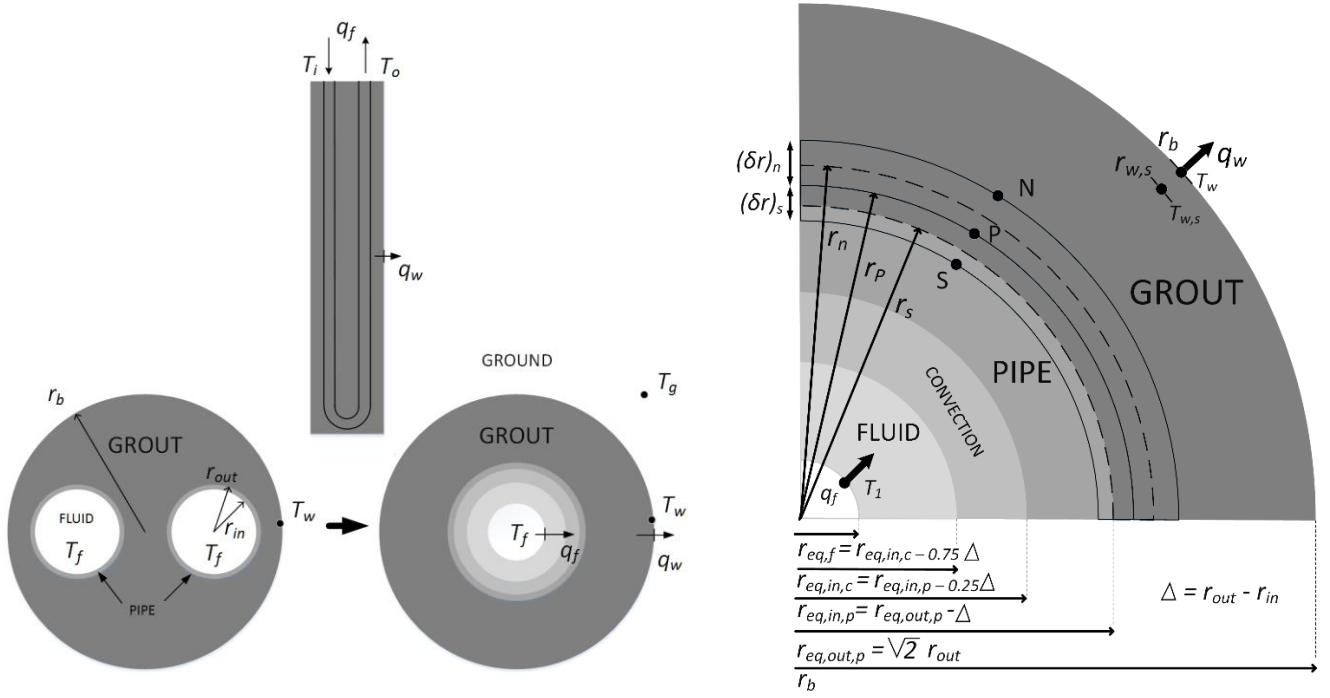
Governing equations and boundary conditions

One-dimensional transient heat transfer in the composite cylinder, is governed by the following equation:

$$\rho C_p \frac{\partial T}{\partial t} = k\frac{1}{r}\frac{\partial}{\partial r}\left(r\frac{\partial T}{\partial r}\right) \tag{2}$$

where ρ, C_p and k are, respectively, the density, specific heat and thermal conductivity. This equation is subjected to the following initial and boundary conditions:

$$T_{t=0} = T_g \quad ; \quad T_{r=r_b} = T_w(t) \quad ; \quad q_{r=r_{eq,f}} = q_f \tag{3}$$

Figure 2 Approximation of the real geometry with an equivalent composite cylinder (left). Dimensions (not to scale) of the various layers and grid layout (right).

Table 1. Equivalent properties for each layer

Layer	Thermal resistance (m-K/W)	Thermal conductivity (W/m-K)	Thermal capacity (ρCp) (kJ/m³-K)
Convection	$R_{eq,c} = \dfrac{1}{2\pi r_{in} h_c n}$	$k_{eq,c} = \dfrac{\ln\left(\dfrac{r_{eq,out,p}}{r_{eq,in,p}}\right)}{2\pi R_{eq,c}}$	Set artificially to a small value
Grout		$k_{eq,gt} = k_{eq,p} = \dfrac{\ln\left(\dfrac{r_b}{r_{eq,in,p}}\right)}{2\pi R_{eq,gt+p}}$	Actual thermal capacity
Pipe	$R_{eq,gt+p} = R_b - R_{eq,c}$		Actual thermal capacity
Fluid	negligible	Set artificially to a high value	See equation 1

eq : equivalent geometry; c : convection; gt : grout; p : pipe

Heat transfer in the composite cylinder geometry is solved using the control-volume method of Patankar (1980) with a fully implicit scheme. Using the nomenclature presented in Figure 2, the discretized equation for an internal node P is given by:

$$a_P T_P = a_N T_N + a_S T_S + b \tag{4}$$

where,

$$a_N = \frac{k_n}{\ln\left(\frac{r_P}{r_{P,n}}\right)} \; ; \; a_S = \frac{k_s}{\ln\left(\frac{r_P}{r_{P,s}}\right)} \qquad ; \; b = a_P^0 T_P^0 \; ; \; a_P = a_P^0 + a_N + a_S \; ; \; a_P^0 = \frac{\rho Cp}{\Delta t}\frac{(r_n^2 - r_s^2)}{2} \tag{4a}$$

The coefficients a_N and a_S, which are different from the traditional formulation (i.e. $a_i = r_i k_i/(\delta r)_i$), are structured so as to account for the logarithmic nature of the temperature profile in a radial configuration. The subscripts "P,s" and "P,n" refer to the nodes immediately upstream and downstream of node P, respectively. The superscript "0" refers to the previous time step and Δt is the time step. Control-volume boundaries are placed at the interface of the different cylinders. The size of the control volumes increases exponentially from the interface to the middle of the layer, then decreases symmetrically until the next interface. Such a configuration prevents inconcistencies due to abrupt temperature changes between two adjacent cylinders with different properties. The boundary condition on the fluid side is entered through the b term for node T_1:

$$b_1 = a_1^0 T_1^0 + r_{eq,f} q_f; \quad \text{where} \quad q_f = r_{eq,f} h_c (T_f - T_1)$$
(4b)

where h_c is the internal convection coefficient. Finally, the borehole wall temperature, T_w, is known at each time step and is given by the infinite cylindrical heat source solution (ICS) to ground heat transfer. The infinite cylindrical heat source (ICS) analytical solution requires the heat transfer rate at the borehole wall, q_w. This value is obtained from the numerical solution of borehole heat transfer as follows:

$$q_w = -2\pi k_{eq,gt} \frac{dT}{dr} \approx -2\pi k_{eq,gt} \frac{T_w - T_{w,s}}{ln\left(\frac{r_b}{r_{w,s}}\right)}$$
(5)

As shown in Figure 2, the subscript "w,s" refers to the node immediately upstream of the last node. In turn, the value of q_w is used to obtain the borehole wall temperature using temporal superposition as follows:

$$T_w - T_g = \sum_{i=1}^{n_t} (q_{w,i} - q_{w,i-1}) \Gamma(t - t_{i-1})$$
(6)

where n_t is the total number of time steps, $\Gamma = \frac{1}{k_g} G(F_o)$ and $F_o = \frac{\alpha_g t}{r_b^2}$

The value of G is the solution of the ICS. It is given here using the approximation provided by Cooper (1976).

Evaluation of short-time g-functions

The evaluation of short-time g-functions is performed as follows. The real borehole geometry is converted into an equivalent composite cylinder (Figure 2) with corresponding properties for each layer (Table 1). Then, the proposed model is solved with a constant value of q_f which is arbitrarily set at 50 W/m in this study. Values of the mean fluid temperature, T_f, and heat transfer at the borehole wall, q_w are then determined at each time step. The short-time g-functions are calculated here based on the work of Yavuzturk and Spitler (1999):

$$g\left(\frac{t}{t_s}, \frac{r_b}{H}\right) = \frac{2\pi k_g (T_f - R_b q_w - T_g)}{q_w}$$
(7)

where t_s is the time scale ($= H^2/9\alpha$)

Grid independence checks

The results of grid independence checks are presented in Figure 3 where short-time g-function values are plotted as a function of $ln(t/t_s)$. The borehole characteristics used for these checks are presented in Table 2. First, the influence of the time step is examined for a fixed number of radial nodes (60). Results for time steps, Δt, of 0.01, 0.05, 0.1, 0.5 and 1 h are reported in Figure 3a. The difference between successive curves diminishes as the Δt is reduced and results for time steps of 0.01 and 0.05 h are very close to each other. A Δt of 0.05 h (3 min.) is a good compromise between computational time and accuracy. It is to be noted that in certain cases it may be required to use a smaller Δt to establish the start of the g-function curve for small values of $ln(t/t_s)$ to capture transient phenomenon occurring over time scales

of seconds. Figure 3b shows the effect of increasing the number of radial nodes from 16 to 60 for a fixed Δt of 0.05 h. The number of nodes is split equally between each of the four cylinders of the equivalent geometry. As shown on Figure 3b, the g-function curve does not change significantly when the number of nodes reaches 40.

Based on this grid independence study, the number of nodes is fixed at 40, i.e.10 nodes per concentric cylinder, and the $\Delta t = 0.05$ h.

One final note regarding Figure 3a, concerns the asymptotic value of the g-function for $t = 0^+$, i.e. for $\ln(t/t_s) \rightarrow -\infty$. For the initial conditions ($t = 0$), $q_w = 0$ and $T_f = T_g$ and according to equation 7, $g = -2\pi k_g R_b$. As show in Figure 3a, this is the asymptotic value of short-time g-functions. A few tests were performed with very small time steps (data not shown on Figure 3) and the proposed method does predict the asymptotic value of the short-time g-function when $t = 0^+$.

Table 2. Borehole characteristics used in Figures 1 and 3

| Borehole characteristics		Layer properties		
Borehole diameter (mm)	108 (100)	**Layer**	**Volumetric heat capacity (kJ/K-m³)**	**Thermal conductivities (W/m-K)**
Borehole total length (m)	108	Fluid	4124	-
U-tube inside diameter (mm)	27.4	Pipe	1540	0.45
U-tube outside diameter (mm)	33.4	Grout	3900	1.280
Shank spacing (mm)	47.1	Ground	2877	2.25
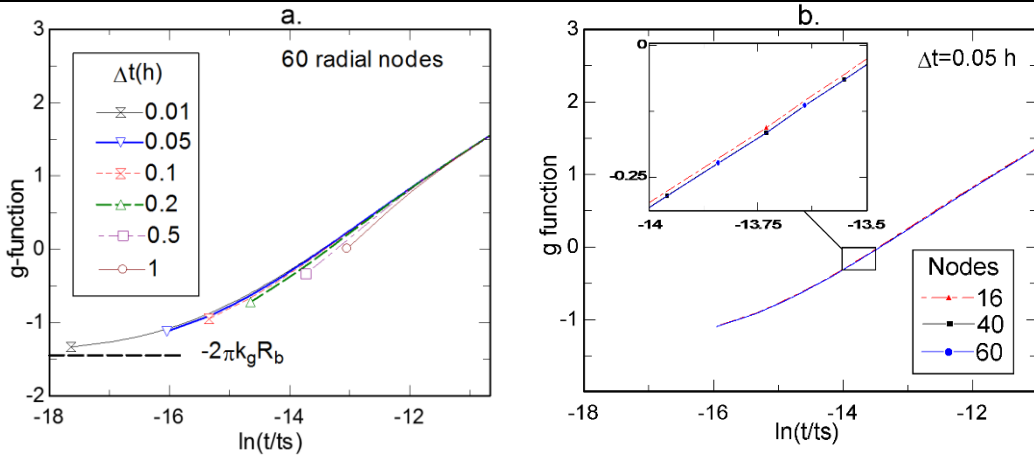
Figure 3 Grid independence checks. a) The number of nodes is fixed at 60 and the time step is varied. b) The time step is fixed at 0.05 h and only number of nodes per layer is varied.

VALIDATION

The proposed model has been validated against several test cases. The first case used test TC3 provided in the building fabric test suite developed by Spitler et al. (2001). This test consists of finding the transient response of a three-layer plane wall. Since the numerical code developed here is for a radial geometry, a large internal radius (1000 m) was used to approximate a plane wall. A fine mesh consisting of 14 nodes per layer and a time-step of 0.02 h were used. The results of this test (not shown here due to a lack of space) indicate that the average relative error on the wall heat flux between the numerical and analytical solution is 0.85%. This comparison indicated that the numerical code was correctly implemented for transient conduction in multi-layer walls.

The experimental data of Beier et al. (2011) is used in the final validation test. The system parameters, geometry and thermal conductivities are taken from Table 1 of Beier et al. (2011). The specific heat capacities for the fluid, pipe, grout and ground are taken as 4.187, 1.77, 3.840, and 3.2 kJ/kg-K, respectively, based on the work of Minaei and Marefat

(2017). The proposed model is used with the experimental values of inlet temperature and flow rate as input. Figure 4 presents the outlet temperature as a function of time predicted by the proposed model and measured by Beier et al. (2011). As shown in the top portion of Figure 4, there is very good agreement between the proposed model and the experiments with maximum and average differences of +0.15 and +0.05 K, respectively.
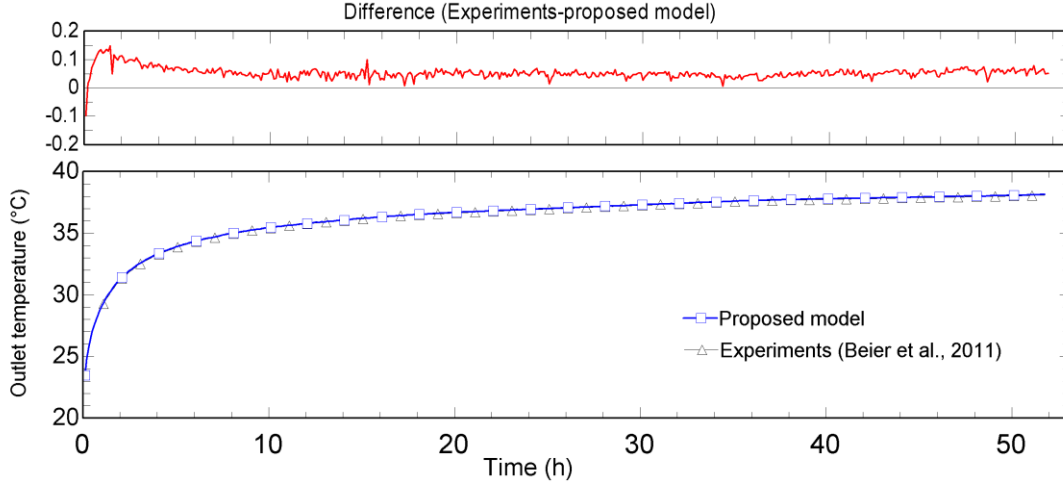
Figure 4 Comparison between the outlet fluid temperature predicted by the proposed model and those measured by Beier et al. (2011).

APPLICATION TO THE ASHRAE SIZING EQUATION

The current ASHRAE sizing equations for vertical boreholes (ASHRAE, 2015) do not account for borehole thermal capacity effects. With short-time g-functions it is possible to account for such effects. When the so-called alternative g-function based design equation (ASHRAE, 2015) is used the required borehole length, L, is given by:

$$L = \frac{q_a R_{ga,g} + q_m R_{gm,g} + q_h R_{gh,g} + q_h R_b}{T_m - T_g} \tag{8}$$

The three ground pulses, q_a, q_m and q_h are applied over time periods which are typically equal to 10 years (t_y), 1 month (t_m), and 1 to 6 hours (t_h), respectively. The corresponding ground thermal resistances, $R_{ga,g}$, $R_{gm,g}$, $R_{gd,g}$ are evaluated as follows (ASHRAE, 2015):

$$R_{ga,g} = \left[g_{(t_f)} - g_{(t_f - t_1)}\right]/2\pi k_g \quad ; \quad R_{gm,g} = \left[g_{(t_f - t_1)} - g_{(t_f - t_2)}\right]/2\pi k_g \quad ; \quad R_{gd,g} = \left[g_{(t_f - t_2)}\right]/2\pi k_g \tag{9}$$

where $t_f = t_y + t_m + t_h$, $t_2 = t_y + t_m$ and $t_1 = t_y$. The subscript "g" denotes that the effective ground thermal resistances are evaluated using g-functions. As noted by Lamarche (2016), short-term g-functions influence the values of $R_{gm,g}$ and $R_{gd,g}$. It is interesting to examine the impact of borehole thermal capacity on the required borehole length for a particular example. In this example, the required length of a single borehole operating in cooling is required for q_a = 0.5 kW, q_m = 3 kW, and q_h=10 kW and t_y = 10 y, t_m =1 month and t_h = 4 hours, and T_m =35 °C and T_g =13 °C. The other borehole characteristics are given in Table 2. The convective heat transfer, h_c, is set at 500 W/m²-K giving a value of R_b = 0.1 m-K/W using the first order multipole method. The corresponding g-function for this geometry is the unified curve for $B/H = \infty$ in Figure 1. Strictly speaking this curve is only applicable for r_b/H=0.0005, thus for a value of H=108 m. Therefore, for different values of the r_b/H ratio, the correction factor suggested by Eskilson is applied. Table 3 presents the required borehole length with and without short-term effects for this case.

Table 3. Short-term effects on borehole length

Parameter	without short-term effects	with short-term effects
Borehole length (m)	109.4	107.3
$R_{ga,g}$ (m-K/W)	0.156	0.155
$R_{gm,g}$ (m-K/W)	0.181	0.187
$R_{gd,g}$ (m-K/W)	0.079	0.072

For this particular example, the design borehole length is slightly oversized ($\approx$ 2%) when short-term effects are not taken into account. Short-term effects decrease the value of $R_{gd,g}$ by about 9 % and increase the value of $R_{gm,g}$ by about 3%. The slight change in the value of $R_{ga,g}$ is not caused directly by borehole thermal capacity but is simply due to the fact that the borehole length varies slightly. The percentage of oversizing is problem dependent and can reach close to 10% (Ahmadfard and Bernier, 2018). It will depend, among other things, on the relative magnitude between q_m and q_h and the duration of the peak pulse.

CONCLUSION

A one-dimensional hybrid model is proposed to generate short-time g-functions for single U-tube boreholes. The two-pipe geometry is first converted into a single equivalent composite cylinder. This cylinder is discretized to numerically solve heat transfer in each layer while ground heat transfer is determined using the infinite cylindrical heat source solution. The influence of the time step and of the number of radial nodes is checked to ensure a good compromise between accuracy and computation time. From this analysis, it appears that 40 nodes and a time step of 3 min is a good compromise between accuracy and computational cost. The numerical part of the model is verified against an analytical solution while the full model is successfully validated against experimental data. Short-time g-functions are generated and used to study the effects of borehole thermal capacity on the required borehole length using the g-function-based ASHRAE sizing equation. It is shown that the inclusion of borehole thermal capacity, using short-time g-functions, reduces the required design borehole length.

NOMENCLATURE

α = thermal diffusivity (m²/s)

B = borehole spacing (m)

q = heat transfer rate per unit length (W/m)

r = radial distance from the borehole center (m)

T = temperature (°C)

k = thermal conductivity (W.m⁻¹.K⁻¹)

a = discretization coefficient (W.m⁻¹.K⁻¹)

δr = node spacing (m)

t = time (h or s)

t_s = time scale (day)

H = borehole length (m)

ρ = density (kg.m⁻³)

C_p = specific heat capacity (J.m⁻³.K⁻¹)

R = effective thermal resistance (m.K.W⁻¹)

Δ = pipe thickness (m)

b = discretization coefficient

Subscripts

b = borehole

gt = grout

eq = equivalent

c = convection

P = node

f = fluid

w = wall

p = pipe

h = hour

s = southern neighbour

n = northern neighbour

a = year

m = month

REFERENCES

Ahmadfard, M. and M. Bernier. 2018. *Modifications to ASHRAE's sizing method for Vertical Ground Heat Exchangers*. Science and Technology for the Built Environment. In press. 2108.

ASHRAE (2015) Chapter 34 – Geothermal Energy, *ASHRAE Handbook - Applications*, Atlanta, GA: ASHRAE.

Bauer, D., W. Heidemann and H.-J.G. Diersch. 2011. *Transient 3d analysis of borehole heat exchanger modeling*. Geothermics 40: 250-260.

Cimmino, M. and M. Bernier. 2013. *Preprocessor for the generation of g-functions used in the simulation of geothermal systems*. Proceedings of the 13th International IBPSA conference, 25-28 August, Chambery, France, pp.2675-2682.

Cimmino, M. and M. Bernier. 2014. *A semi-analytical method to generate g-functions for geothermal bore fields*. Int. J. Heat Mass Transfer 70(c): 641-650.

Claesson, J. and S. Javed. 2011. *An analytical method to calculate borehole fluid temperatures for time-scales from minutes to decades*. ASHRAE annual conference, paper ML-11-C034.

Cooper, L.Y. 1976. *Heating of a Cylindrical Cavity*. International Journal of Heat and Mass Transfer 19: 575-577.

Eskilson, P. 1987. *Thermal analysis of heat extraction boreholes*. University of Lund, Sweden: Doctoral Thesis.

Javed, S., J. Claesson and P. Fahlén. 2010. *Analytical Modelling of Short-term Response of Ground Heat Exchangers in Ground Source Heat Pump Systems*. 10th REHVA World Congress, Clima 2010, Antalya, Turkey, May 9-12.

Javed, S. and J. Claesson. 2011. *New analytical and numerical solutions for the short-term analysis of vertical ground heat exchangers*. ASHRAE Transaction 117(1): 3-12.

Kim, E.-J., M. Bernier, O. Cauret and J.-J. Roux. 2014. *A hybrid reduced model for borehole heat exchangers over different time-scales and regions*. Energy 77: 318-326.

Lamarche, L. 2015. *Short-time analysis of vertical boreholes, new analytic solutions and choice of equivalent radius*. International Journal of Heat and Mass Transfer 91: 800-807.

Lamarche, L. 2016. *Short-time modelling of geothermal systems*. 29th internation conference on efficiency, cost, optimization, simulation and environmental impact of energy systems, Portoroz, Slovenia, June 19-23, Proceedings.

Li, M. and A. C. Lai. 2013. *Analytical model for short-time responses of ground heat exchangers with U-shaped tubes: Model development and validation*. Applied Energy 104: 510-516.

Li, M., P. Li, V.Chan and A. C. Lai. 2014. *Full-scale temperature response function (G-function) for heat transfer by borehole ground heat exchangers (GHEs) from sub-hour to decades*. Applied Energy 136: 197-205.

Ma, W., M. Li, P. Li and A. C. Lai. 2015. *New quasi-3D model for heat transfer in U-shaped GHEs (ground heat exchangers): Effective overall thermal resistance* Energy 90: 578-587.

Pärisch, P., O. Mercker, P. Oberdorfer, E. Bertram, R. Tepe. and G. Rockendorf. 2015. *Short-term experiments with borehole heat exchangers and model validation in TRNSYS*. Renewable Energy 74: 471-477.

Rees, S. J. 2015. *An extended two-dimensional borehole heat exchanger model for simulation of short and medium timescale thermal response*. Renewable Energy 83: 518-526.

Ruiz-Calvo, F., M. De Rosa, P. Monzo, C. Montagud and J. Corberan. 2016. *Coupling short-term (B2G model) and long-term (g-function) models for ground heat exchanger simulation in TRNSYS. Application in a real installation*. App.Thermal Eng102: 720-732.

Ruiz-Calvo, F., De Rosa, M., Acuña, J., Corberán, J. and C. Montagud. 2015. *Experimental validation of a short-term Borehole-to-Ground (B2G) dynamic model*. Applied Energy 140: 210-223.

Shirazi, A. S. and M. Bernier. 2013. *Thermal capacity effects in borehole ground heat exchangers*. Energy and Buildings 67: 352-364.

Shonder, J.A. and J.V. Beck. 1999. *Determining effective soil formation thermal properties from field data using a parameter estimation technique*. ASHRAE Transactions 105: 458-468.

Spitler, J. D., S.J. Rees and X. Dongyi. 2001. *Development of an analytical verification test suite for whole building energy simulation program - building fabric*. ASHRAE 1052-RP: Final Report.

Spitler, J. D. and X. Xu . 2006. *Modeling of Vertical Ground Loop Heat Exchangers with Variable Convective Resistance and Thermal Mass of the Fluid*. Proceedings of the 10th Int. Conference on Thermal Energy Storage-Ecostock 2006, Pomona, NJ.

Yang, Y. and M. Li. 2014. *Short-time performance of composite-medium line-source model for predicting responses of ground heat exchangers with single U-shaped tube*. International Journal of Thermal Sciences 82: 130-137.

Yavuzturk, C. and J.D. Spitler. 1999. *A short time step response factor model for vertical ground loop heat exchangers*. ASHRAE Transactions. 105(2): 475-485.

Yavuzturk, C. and J.D. Spitler. 2001. *Field validation of a short time step model for vertical ground-loop heat exchangers*. ASHRAE Transactions 107(1):617-625.